

# The Top Forward Backward Asymmetry with general $Z'$ couplings

Murugeswaran Duraisamy <sup>†</sup>, Ahmed Rashed <sup>†,‡</sup>, and Alakabha Datta <sup>†</sup>

<sup>†</sup> *Department of Physics and Astronomy,  
University of Mississippi,  
Lewis Hall, University, Mississippi, 38677, USA*

<sup>‡</sup> *Department of Physics,  
Ain Shams University,  
Faculty of Science, Cairo, 11566, Egypt*

(Dated: February 24, 2024)

The measurement of the top forward-backward asymmetry in  $t\bar{t}$  production measured at the Tevatron shows deviation from the standard model prediction. A  $u \rightarrow t$  transition via a flavor-changing  $Z'$  can explain the data. We show that left-handed  $t_L u_L Z'$  couplings can be constrained from  $B_{d,s}$  mixing while the constraints on the right-handed couplings  $t_R u_R Z'$  vanish in the limit of  $m_u \rightarrow 0$ . We then consider the most general form of the  $tuZ'$  interaction which includes vector-axial vector as well as tensor type couplings and study how these couplings affect the top forward-backward asymmetry.

PACS numbers:

The top quark with its high mass may play a crucial role in electroweak symmetry breaking. Hence the top sector may be sensitive to new physics (NP) effects that could be revealed through careful measurements of top quark properties. The top quark pair production in proton-antiproton collisions at the Tevatron collider with a center-of-mass energy of  $\sqrt{s} = 1.96$  TeV is dominated by the partonic process  $q\bar{q} \rightarrow t\bar{t}$ . Recently the CDF experiment has reported a measurement of forward-backward asymmetry in  $t\bar{t}$  production which appears to deviate from the standard model (SM) predictions. The CDF collaboration measured the forward-backward asymmetry ( $A_{FB}$ ) in top quark pair production in the  $t\bar{t}$  rest frame to be  $A_{FB}^{t\bar{t}} = 0.475 \pm 0.774$  for  $M_{t\bar{t}} > 450$  GeV [1], which is 3.4  $\sigma$  deviations from the next-to leading order (NLO) SM prediction  $A_{FB}^{t\bar{t}} = 0.088 \pm 0.013$  [2–5]. The DØ collaboration also observed a larger than predicted asymmetry [6].

The current measurement of the top quark pair production cross section from 4.6 fb<sup>-1</sup> of data at CDF is

$$\sigma_{t\bar{t}} = (7.50 \pm 0.48) \text{ pb}, \quad (1)$$

for  $m_t = 172.5$  GeV [7], in good agreement with their SM predictions by Langenfeld *et al.*  $\sigma_{t\bar{t}} = 7.46^{+0.66}_{-0.80}$  pb [8], Cacciari *et al.*  $\sigma_{t\bar{t}} = 7.26^{+0.78}_{-0.86}$  pb [9], Kidonakis  $\sigma_{t\bar{t}} = 7.29^{+0.79}_{-0.85}$  pb [10], and recent Ahrens *et al.*'s significantly low value  $\sigma_{t\bar{t}} = 6.30 \pm 0.19^{+0.31}_{-0.23}$  pb [11]. Hence new physics models that aim to explain the  $A_{FB}$  measurement must not change the production cross section appreciably. Many NP models that affect  $A_{FB}$ , either via s-channel [12–30] or  $t$ -channel exchange of new particles [31–57] have been proposed to explain the forward-backward anomaly. Here we will focus on the model with a  $Z'$  boson that has a flavor-changing  $tuZ'$  coupling. This coupling can contribute to  $t\bar{t}$  production at the Tevatron via the  $t$ -channel exchange of the  $Z'$  boson (see Fig. 1(a)). The  $A_{FB}$  measurement can be explained with a light  $Z'$  with a mass around

150 GeV and flavor-changing  $tuZ'$  coupling of  $g_{utZ'} \sim O(g)$  where  $g$  is the weak coupling. One can take higher  $Z'$  masses which requires larger  $g_{utZ'} \geq 1$  values [58].

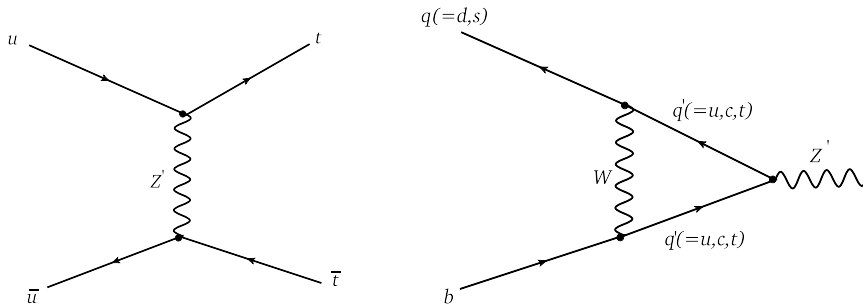


FIG. 1: Left panel(a): Tree-level  $t\bar{t}$  production diagram involving the  $Z'$  exchange. Right panel(b): Tree-level diagram with  $tq'Z'$  coupling ( $q' = u, c, t$ ) which generates an effective  $bqZ'$  ( $q = d, s$ ) coupling through a vertex correction involving the  $W$  exchange.

Flavor-changing neutral current (FCNC) effects in the SM are tiny and satisfy the condition of natural flavor conservation proposed by Glashow, Weinberg and Paschos [59]. The condition of natural flavor conservation can be avoided if quarks of the same charge couple to more than one Higgs or their couplings to a new vector boson (e.g. a  $Z'$  boson) are different for different generation. To date there is no experimental evidence of FCNC effects beyond those expected from the SM. There are some anomalies in the  $B$  system which might require new physics to resolve, but the NP-generated FCNC effects that are needed in the  $B$  system are much smaller than the one needed to resolve the top  $A_{FB}$  [60]. A tree-level  $dbZ'$  or a  $sbZ'$  coupling is strongly suppressed by  $B_{d,s}$  mixing. A tree-level  $tq'Z'$  coupling, where  $q' = u, c, t$ , will generate an effective  $bqZ'$  ( $q = d, s$ ) coupling through a vertex correction involving the  $W$  exchange [61] (see Fig. 1(b)). The  $B_q$  mixing constraints on these effective vertices would then lead to constraints on the  $tq'Z'$  coupling. The vertex corrections are divergent and can be regulated by a cut off  $\Lambda$ , which represents the scale of NP in an effective theory framework. In NP models where there are no bare  $bqZ'$  couplings, the vertex corrections with a chosen  $\Lambda$  can be used to constrain the  $tq'Z'$  coupling from  $B_q$  mixing measurements. We will take the scale of new physics to be  $\sim TeV$ . In specific complete models  $\Lambda$  will represent the mass of some new particles. In models of NP where there are bare  $bqZ'$  couplings the vertex correction will renormalize the bare  $bqZ'$  vertices to produce the renormalized vertices  $U_{qb}$ . These renormalized vertices can then be fitted to  $B_q$  mixing data. Assuming the vertex corrections to be less than or at most the same size of the bare couplings one, we can obtain bounds on the  $tqZ'$  couplings by requiring the generated  $bqZ'$  coupling to be  $\leq U_{qb}$ . It is possible to have models where large bare  $bqZ'$  couplings cancel with large vertex corrections to produce small renormalized  $bqZ'$  vertices consistent with experiments. We will not consider these finely tuned model.

When the vertex corrections are computed, one finds that right-handed  $tuZ'$  couplings do not contribute to  $B_q$  mixing in the limit of setting the up quark mass to zero. We note that  $ttZ'$  couplings do not have such suppression and will contribute to  $B_q$  mixing via the vertex corrections. Even though the  $ttZ'$  coupling does not contribute to the top  $A_{FB}$ , in specific models of NP this coupling may be related to the FCNC coupling  $tuZ'$  [62]. It turns out the  $B_q$  mixing constraints on  $ttZ'$  are weak because of the small Cabibbo-Kobayashi-Maskawa (CKM) matrix elements  $V_{ts(d)}$  and not because of right-handed couplings. The  $tqZ'$  ( $q = u, c, t$ ) couplings via box diagrams can produce an effective  $\bar{d}(\bar{s})b\bar{u}u$  operator that can contribute to decays like  $B \rightarrow K(K^*)\pi(\eta, \eta'\rho)$  or  $B \rightarrow \pi(\rho)\pi(\rho)$ , etc. decays. The effects of these new operators can be observed in CP-violating and/or triple product measurements [63]. However, these effective operators only modify the SM Wilson's coefficients in the SM effective Hamiltonian and so the CP-violating predictions and/or triple

product measurements should be similar to the SM for a reasonable choice of  $tqZ'(q = u, c, t)$  couplings.

We will next consider the most general  $tuZ'$  couplings including both vector, axial vector and tensor couplings ( $\sim \frac{\sigma_{\mu\nu} q^\nu}{m_t}$ ) and study the effect of these couplings on the top  $A_{FB}$ . The interesting feature about these tensor couplings are that we can avoid the  $B_q$  mixing constraints due to the suppressions of these operators at low energies [64]. The momentum dependence of these operators imply that at the b quark scale these operators will be suppressed by  $\sim m_b/m_t$  and consequently the  $B_q$  mixing constraints will be weak for these operators.

The paper is organized in the following manner. In the next section we discuss the  $B_q(q = d, s)$  constraints on the  $tuZ'$  operators. In the following section we introduce the general  $tuZ'$  coupling including tensor terms and study the effects in the top  $A_{FB}$ . This is followed by the section on the  $t \rightarrow uZ'$  branching ratio calculations. In the final section we present our conclusions.

## I. CONSTRAINTS ON $tq'(=u, t)Z'$ COUPLINGS FROM $B_{q(=d,s)}$ MIXING

In general, new physics contributions to the mass difference between neutral  $B_q$  meson mass eigenstates ( $\Delta M_q$ ) can be constrained by the  $\Delta M_q$  experimental results. In the SM,  $B_q^0-\bar{B}_q^0$  mixing occurs at the one-loop level by the flavor-changing weak interaction box diagrams. The mixing amplitude  $M_{12}^q$  is related to the mass difference  $\Delta M_q$  via  $\Delta M_q = 2|M_{12}^q|$ . The recent theoretical estimations for the mass differences of  $B_s^0-\bar{B}_s^0$  and  $B_d^0-\bar{B}_d^0$  mixing [65] at  $1\sigma$  confidence level are

$$(\Delta M_s)^{SM} = 16.8_{-1.5}^{+2.6} \text{ ps}^{-1}, \quad (\Delta M_d)^{SM} = 0.555_{-0.046}^{+0.073} \text{ ps}^{-1}. \quad (2)$$

The latest measurements of mass difference by CDF [66] and DØ [67] for  $B_s$  mixing are

$$\begin{aligned} \Delta M_{B_s} &= (17.77 \pm 0.10(\text{stat.}) \pm 0.07(\text{syst.})) \text{ ps}^{-1} \\ \Delta M_{B_s} &= (18.53 \pm 0.93(\text{stat.}) \pm 0.30(\text{syst.})) \text{ ps}^{-1}. \end{aligned} \quad (3)$$

The Heavy Flavor Averaging Group value for the mass difference of  $B_d^0-\bar{B}_d^0$  mixing is  $\Delta M_{B_d}(\text{exp}) = (0.507 \pm 0.004) \text{ ps}^{-1}$  [68]. The experimental results for the mass differences of both  $B_s^0-\bar{B}_s^0$  and  $B_d^0-\bar{B}_d^0$  mixing are consistent with their SM expectations. Hence, the mass difference results can provide strong constraints on NP contributions.

In this section we will consider the  $B_{d,s}$  mixing constraints on the  $tq'(=u, t)Z'$  couplings.

### 1. $tuZ'$ left-handed coupling

The most general Lagrangian for flavor-changing  $tuZ'$  transition is [69]

$$\mathcal{L}_{tuZ'} = \bar{u} \left[ \gamma^\mu (a + b\gamma_5) + i \frac{\sigma_{\mu\nu} q^\nu}{m_t} (c + d\gamma_5) \right] t Z'_\mu, \quad (4)$$

where  $q = p_t - p_u$ . In general, the couplings a, b, c and d are complex and can be momentum-dependent (form factors). In this work we will take the couplings to be constants with no momentum dependence. Consider the  $tuZ'$  vertex with  $a = -b = g_{tu}^L$ , and  $c=d=0$  in Eq. (4). This generates effective  $bqZ'(q = d, s)$  coupling at one-loop level due to W exchange. We obtain the  $bqZ'$  coupling in the Pauli-Villars regularization as

$$\mathcal{L}_{Z'} = U_{qb} \bar{q} \gamma^\mu (1 - \gamma_5) b Z'_\mu, \quad (5)$$

where

$$U_{qb} = g_{tu}^L \frac{G_F}{\sqrt{2}} M_W^2 (V_{uq}^* V_{tb} + V_{tq}^* V_{ub}) \frac{1}{8\pi^2} \left[ \frac{x_t \text{Log}[\frac{\Lambda^2}{\bar{m}_t^2}] - \text{Log}[\frac{\Lambda^2}{M_W^2}]}{(x_t - 1)} \right]. \quad (6)$$

where  $\Lambda \sim \text{TeV}$  is a cutoff scale, and  $x_t = m_t^2/M_W^2$ . The function  $U_{qb}$  includes only the contribution from the W boson, and the contribution of the associated Goldstone boson in the SM is the order of  $m_u/M_W$ . Note that for  $B_d$  mixing the coupling  $g_{tu}^L$  is associated with the CKM factor  $V_{ud}^* V_{tb} \sim 1$ , and thus one can expect a strong constraint on  $g_{tu}^L$  from the mass difference  $\Delta M_d$ .

A tree-level exchange of the  $Z'$  generates the  $\Delta B = 2$  effective Lagrangian responsible for the neutral  $B_q$  meson mixing

$$\mathcal{H}_{Z'}^{\Delta B=2} = \frac{U_{qb}^2}{M_{Z'}^2} \eta_{Z'} (\bar{q}b)_{V-A} (\bar{q}b)_{V-A}, \quad (7)$$

where  $(\bar{q}b)_{V-A} = \bar{q}\gamma^\mu(1 - \gamma_5)b$ , and the QCD correction factor  $\eta_{Z'} = [\alpha_s(M_{Z'})/\alpha_s(m_b)]^{6/23}$ . The  $Z'$  contribution to the  $B_q$  mixing amplitude can be obtained by using the vacuum insertion method as

$$[M_{12}^q]^{Z'} = \frac{4}{3} \frac{U_{qb}^2}{M_{Z'}^2} \eta_{Z'} m_{B_q} f_{B_q}^2 B_q. \quad (8)$$

In the presence of new physics, the mixing amplitude  $M_{12}^q$  can be parameterized by complex parameters  $\Delta_q$  [65]

$$M_{12}^q = [M_{12}^q]^{SM} \Delta_q. \quad (9)$$

In our case,  $\Delta_q = |\Delta_q| e^{i\phi_q^\Delta} = 1 + [M_{12}^q]^{Z'}/[M_{12}^q]^{SM}$ . A global analysis on the parameters  $|\Delta_q|$  and  $\phi_q^\Delta$  for  $B_d - \bar{B}_d$  and  $B_s - \bar{B}_s$  mixing are carried out in [65]. The best fit results for  $\Delta_d$  and  $\Delta_s$  in this analysis at 1  $\sigma$  confidence level (scenario I) are

$$|\Delta_d| = 0.747_{-0.082}^{+0.195}, \quad \phi_d^\Delta = -12.9_{-2.7}^{+3.8^\circ}, \quad (10)$$

and

$$|\Delta_s| = 0.887_{-0.064}^{+0.143}, \quad \phi_s^\Delta = -51.6_{-9.7}^{+14.2^\circ} \quad \text{or} \quad -130.0_{-12}^{+13^\circ}. \quad (11)$$

The  $\Delta_d$  constraint in Eq. (10) on the coupling  $g_{tu}^L$  at  $\bar{m}_t(\bar{m}_t) = (165.017 \pm 1.156 \pm 0.11) \text{ GeV}$  [65],  $\beta^{SM} = 27.2_{-3.1}^{+1.1^\circ}$  [65], and  $M_{Z'} = 150 \text{ GeV}$  is shown in Fig. 2. The numerical values of all other theoretical inputs can be found in [65]. They are varied within 1  $\sigma$  errors in the fit. The cutoff scale  $\Lambda$  is varied between 300 GeV to 2 TeV. The green scatter points in Fig. 2 satisfy only  $|\Delta_d|$  in Eq. (10), while blue points satisfy both  $|\Delta_d|$  and  $\phi_d^\Delta$  in Eq. (10). The results indicates that  $B_d$  mixing can strongly constrain the  $tuZ'$  coupling  $g_{tu}^L$  even at  $\Lambda = 300 \text{ GeV}$ . In particular we note that the maximum value for  $|g_{tu}^L|$  is around 0.2 and is associated with a large phase. In fact there are no real  $g_{tu}^L$  that satisfy the  $B_d$  constraint.

On the other hand, Fig. 3 suggests that the constraints from  $B_s$  mixing on the  $tuZ'$  coupling  $g_{tu}^L$  are weaker ( $\sim O(1)$ ) even at  $\Lambda = 2 \text{ TeV}$ . This can be understood from the fact that the  $B_s$  mixing contribution in this case is associated with the CKM factor  $V_{us}^* V_{tb}$  and is suppressed. The (green, blue, red) scatter points in Fig. 3 are constrained by ( $|\Delta_s|$ ,  $\{|\Delta_s|, \phi_s^\Delta = -51.6_{-9.7}^{+14.2^\circ}\}$ ,  $\{|\Delta_s|, \phi_s^\Delta = -130.0_{-12}^{+13^\circ}\}$ ) in Eq. (11), respectively. The large negative phase  $\phi_s^\Delta$  prefers large  $g_{tu}^L$  values.

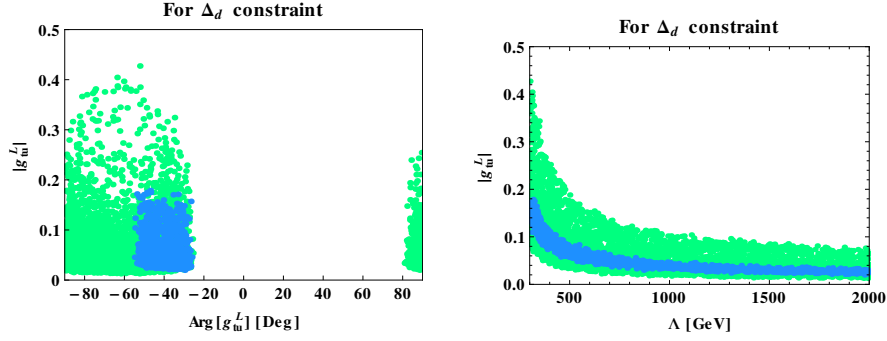


FIG. 2:  $|g_{tu}^L|$  vs  $\text{Arg}[g_{tu}^L][\text{Deg}]$  (left panel) and  $|g_{tu}^L|$  vs  $\Lambda[\text{GeV}]$  (right panel) for  $B_d$  mixing. Green scatter points are constrained by  $|\Delta_d|$ . Blue scatter points are constrained by  $|\Delta_d|$  and  $\phi_d^\Delta$ .

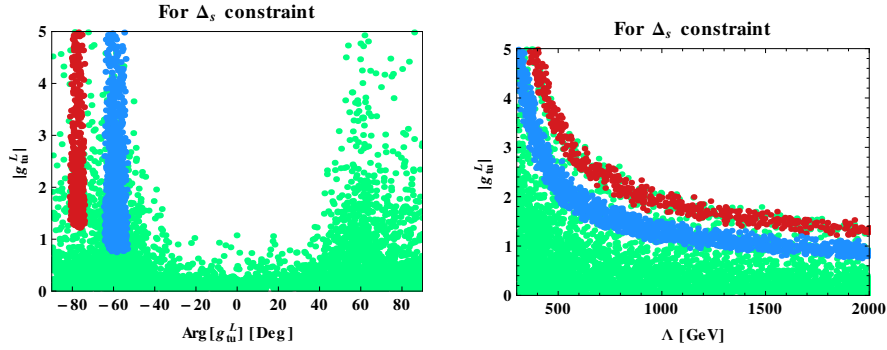


FIG. 3:  $|g_{tu}^L|$  vs  $\text{Arg}[g_{tu}^L][\text{Deg}]$  (left panel) and  $|g_{tu}^L|$  vs  $\Lambda[\text{GeV}]$  (right panel) for  $B_s$  mixing. Green scatter points are constrained by  $|\Delta_s|$ . Blue scatter points are constrained by  $|\Delta_d|$  and  $\phi_d^\Delta = -51.6^{+14.2^\circ}_{-9.7^\circ}$ . Red scatter points are constrained by  $|\Delta_d|$  and  $\phi_d^\Delta = -130.0^{+13^\circ}_{-12^\circ}$ .

## 2. $tuZ'$ right-handed coupling

We now consider the  $tuZ'$  vertex with right-handed couplings,  $a = b = g_R$ , and  $c=d=0$ . The contribution of this vertex to  $M_{12}$  is suppressed by  $m_u^2/m_W^2$ . Hence, the right-handed coupling  $g_R$  cannot be constrained by  $B_q$  mixing.

Finally as indicated in the earlier section, the left- and the right-handed couplings generate via the box diagram effective  $\bar{q}b\bar{u}u$  ( $q = d, s$ ) operators. These operator can be constrained by observables in nonleptonic B meson decays like  $B \rightarrow \pi\pi/K\pi$ . These operators change the Wilson's coefficients of the SM effective Hamiltonian with the change being  $\sim 10^{-2}$  at the scale  $\mu = M_W$  for  $M_{Z'} = 150 \text{ GeV}$  and  $g_{tu}^L, g_{tu}^R \sim O(g)$ . Since the generated NP physics operator structures are similar to the SM there are no easy way to detect their presence. A detailed fit to all the nonleptonic data may provide constraints on the couplings  $g_{tu}^{L,R}$ , which we do not perform in this work. Some analysis along this line has been done for  $tdW'$  coupling in [70].

## 3. $ttZ'$ coupling

For completeness, next we consider  $B_q$  mixing constraints on the  $ttZ'$  couplings. The Lagrangian for the  $ttZ'$  interaction is

$$\mathcal{L}_{ttZ'} = \bar{t}[g_{tt}^L\gamma^\mu(1 - \gamma_5) + g_{tt}^R\gamma^\mu(1 + \gamma_5)]tZ'_\mu. \quad (12)$$

Again, we evaluate the one-loop diagram (see Fig. 1(b)) in the Pauli-Villars regularization and obtain the effective Lagrangian for  $bq(=d,s)Z'$  interaction as

$$\mathcal{L}'_{Z'} = U'_{qb} \bar{q} \gamma^\mu (1 - \gamma_5) b Z'_\mu, \quad (13)$$

where

$$U'_{qb} = \frac{G_F}{\sqrt{2}} M_W^2 V_{tq} V_{tb} f_{tt}(\Lambda, x_t), \quad (14)$$

with

$$f_{tt}(\Lambda, x_t) = \frac{1}{(4\pi^2)} \int_0^1 dx \int_0^{1-y} dy \left[ g_{tt}^L \left( \text{Log} \left[ \frac{x\Lambda^2}{M_W^2 D_{tt}} \right] + \frac{1}{2} \frac{x_t^2}{D_{tt}} \right) + g_{tt}^R x_t \left( \frac{1}{2} \text{Log} \left[ \frac{x\Lambda^2}{M_W^2 D_{tt}} \right] + \frac{1}{D_{tt}} \right) \right], \quad (15)$$

and  $D_{tt} = x + (1-x)x_t$ . The function  $f_{tt}$  includes both the W boson and the associated Goldstone boson contributions. The  $ttZ'$  contribution to the  $B_q$  mixing amplitude is

$$[M_{12}^q]^{Z'} = \frac{4}{3} \frac{[U'_{qb}]^2}{M_{Z'}^2} \eta_{Z'} m_{B_q} f_{B_q}^2 B_q. \quad (16)$$

Both  $B_d - \bar{B}_d$  and  $B_s - \bar{B}_s$  constraints in Eqs. (10) and (11) can allow large  $\sim O(1)$  values for  $g_{tt}^{L,R}$ .

## II. TOP QUARK FORWARD-BACKWARD ASYMMETRY

In this section we calculate the top  $A_{FB}$  keeping in mind the constraints derived on the coupling from the previous section. The most general Lagrangian for a flavor-changing  $tuZ'$  interaction is given in Eq. (4). This interaction can contribute to  $u\bar{u} \rightarrow t\bar{t}$  scattering amplitude through the t-channel exchange of the  $Z'$  boson (see Fig. 1(a)). The tree-level differential cross section for  $q\bar{q} \rightarrow t\bar{t}$  process in the  $t\bar{t}$  center-of-mass frame including both the SM and for  $Z'$  contributions is

$$\frac{d\hat{\sigma}}{d\cos\theta} = \frac{\beta_t}{32\pi\hat{s}} (\mathcal{A}_{SM} + \mathcal{A}_{SM-Z'} + \mathcal{A}_{Z'}), \quad (17)$$

where  $\hat{s} = (p_q + p_{\bar{q}})^2$  is the squared center-of-mass energy of the  $t\bar{t}$  system,  $\beta_t = \sqrt{1 - 4m_t^2/\hat{s}}$ , and the polar angle  $\theta$  is the relative angle between direction of motion of the outgoing top quark and the incoming q quark. The quantities  $\mathcal{A}_{SM}$ ,  $\mathcal{A}_{SM-Z'}$ , and  $\mathcal{A}_{Z'}$  denote the leading order SM, the interference between the SM and  $Z'$ , and the pure  $Z'$  scattering amplitudes, respectively. These amplitudes can be obtained in terms of kinematic variables  $\theta$  and  $\hat{s}$  as

$$\begin{aligned} \mathcal{A}_{SM} &= \frac{2g_s^4}{9} \left[ 1 + c_\theta^2 + \frac{4m_t^2}{\hat{s}} \right], \\ \mathcal{A}_{SM-Z'} &= \frac{2g_s^2}{9} \left[ \frac{\hat{t} - M_{Z'}^2}{(\hat{t} - M_{Z'}^2)^2 + M_{Z'}^2 \Gamma_{Z'}^2} \right] (f_1 + f_2), \\ \mathcal{A}_{Z'} &= \frac{1}{4} \left[ \frac{1}{(\hat{t} - M_{Z'}^2)^2 + M_{Z'}^2 \Gamma_{Z'}^2} \right] (f_3 + f_4 + f_5). \end{aligned} \quad (18)$$

Where  $c_\theta = \beta_t \cos\theta$ , and  $\hat{t} = (p_q - p_t)^2 = -\hat{s}/2(1 - \beta_t \cos\theta) + m_t^2$ . The functions  $f_i$ s (i = 1-5) can be found in the Appendix. Here we assume the couplings a, b, c and d to be real. Our results for  $t\bar{t}$  production are obtained by the convolution of the analytic differential cross section of Eq. (17) with the CTEQ-5L

parton distribution functions [71] implemented in Mathematica. We expect the MSTW 2008 [72] parton distributions to give compatible results.

The forward-backward asymmetry of the top quark in the  $t\bar{t}$  c.m. frame is defined as [73]

$$A_{FB}^{t\bar{t}} = \frac{\sigma_F - \sigma_B}{\sigma_F + \sigma_B}, \quad (19)$$

where

$$\sigma_F = \int_0^1 \frac{d\sigma}{d\cos\theta} d\cos\theta, \quad \sigma_B = \int_{-1}^0 \frac{d\sigma}{d\cos\theta} d\cos\theta. \quad (20)$$

In our analysis, we choose some representative values for the couplings  $a$ ,  $b$ ,  $c$ , and  $d$  to generate large forward-backward asymmetry  $A_{FB}^{t\bar{t}}$  for high  $M_{t\bar{t}}$  ( $> 450$  GeV) without distorting the shape of the mass spectrum  $d\sigma_{t\bar{t}}/dM_{t\bar{t}}$ . We fix the renormalization and factorization scales at  $\mu_R = \mu_F = m_t$ . We evaluate  $A_{FB}^{t\bar{t}}$  which includes the NLO SM and the  $Z'$  contributions at  $m_t = 172.5$  GeV. Also, we apply a QCD K-factor  $K = 1.3$  to the tree-level cross section in order to match the SM prediction for  $\sigma_{t\bar{t}}$ . We consider the  $Z'$  boson with mass  $M_{Z'} = 150$  GeV and width  $\Gamma_{Z'} = 0$  for the numerical analysis.

#### A. Pure vector-axial vector couplings: $a = \mp b$ and $c = d = 0$

This case has already been considered before [31], but only right-handed couplings were considered. Here we will consider both right- and left-handed couplings. We take the representative values of the couplings  $a = -b = |g_{tu}^L| = 0.257$ , and  $c = d = 0$ . This value for  $g_{tu}^L$  satisfies the  $|\Delta_d|$  constraint but not the phase  $\phi_d^\Delta$  constraints from  $B_d$  mixing (see Fig. 2). For these values  $A_{FB}^{t\bar{t}}$  can be explained within one  $\sigma$  error of its measurement for  $M_{t\bar{t}} > 450$  GeV. In Fig. 4, we show the  $M_{t\bar{t}}$  distribution for the  $t\bar{t}$  observables  $A_{FB}^{t\bar{t}}$ , and  $\sigma_{t\bar{t}}$ . The differential distribution,  $d\sigma_{t\bar{t}}/dM_{t\bar{t}}$ , has been measured in eight different energy bins of  $M_{t\bar{t}}$  for  $m_t = 175$  GeV in Ref. [74]. Our distribution of  $d\sigma_{t\bar{t}}/dM_{t\bar{t}}$  is consistent with the measurements. Since the partonic scattering amplitudes in this case (see the Appendix) depends on  $b^2$  and  $b^4$  terms, our results hold for right-handed couplings also, i.e  $a = b = |g_{tu}^R| = 0.257$ , and  $c = d = 0$ .

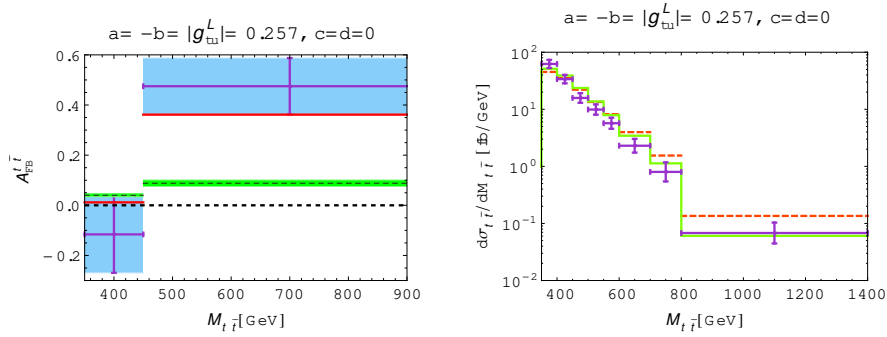


FIG. 4: Left panel:  $M_{t\bar{t}}$  distribution of  $A_{FB}^{t\bar{t}}$  in the two energy ranges [350,450]GeV and [450,900]GeV of invariant mass  $M_{t\bar{t}}$ . Green band: the SM prediction. Blue band with  $1\sigma$  error bars: the unfolded CDF measurement [1]. Red line: the SM with  $Z'$  exchange prediction for  $(a = -b = 0.257, c = d = 0)$ . Right panel:  $M_{t\bar{t}}$  distribution of  $d\sigma_{t\bar{t}}/dM_{t\bar{t}}$  [in fb/GeV] for eight different energy bins of  $M_{t\bar{t}}$ . Green line: the NLO SM prediction. Blue band with  $1\sigma$  error bars: the unfolded CDF measurement [74]. Red line: the SM with  $Z'$  exchange prediction for above values of couplings at  $m_t = 175$  GeV.

### B. General case: all couplings are present

In this section we consider the most general  $tuZ'$  couplings. We showed earlier that the left-handed coupling are strongly constrained from  $B_d$  mixing and there are no real values of  $g_{tu}^L$  that satisfy the  $B_d$  mixing constraint. We now investigate the effect of the couplings  $c$  and  $d$  on the  $A_{FB}$  predictions.

### C. Pure tensor couplings : $a = b = 0$ and $c = \pm d$

We consider the case of pure tensor couplings. In this scenario we can avoid the  $B_q$  mixing constraints as the effects of the tensor couplings are suppressed by  $\frac{m_b}{m_t}$  at the  $b$  mass scale. The SM and  $Z'$  interference contribution  $\mathcal{A}_{SM-Z'}$  in Eq. (18) vanishes in this case. The functions  $f_4$  and  $f_5$  in pure  $Z'$  contribution  $\mathcal{A}_{Z'}$  are also zero, and  $f_3$  is order of  $(c\hat{s}/m_t)^2$ . The mass spectrum for  $A_{FB}^{t\bar{t}}$  is shown in Fig. 5(a) for only  $c = \pm d$  couplings ( $c = \pm d = 0.5$ ). The results indicate that  $Z'$  contribution cannot reproduce the  $A_{FB}$  measurement within one  $\sigma$  for  $M_{t\bar{t}} > 450$  GeV even at a low  $M_{Z'} = 100$  GeV (yellow lines) value.

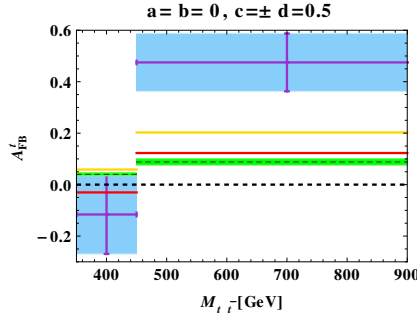


FIG. 5:  $M_{t\bar{t}}$  distribution of  $A_{FB}^{t\bar{t}}$ . Green band: The SM prediction. Blue band with  $1\sigma$  error bars : CDF measurement. Red and yellow lines: The SM with  $Z'$  exchange prediction at  $M_{Z'} = 150$  GeV, and  $M_{Z'} = 100$  GeV, respectively, for  $a = b = 0$  and  $c = \pm d = 0.5$ .

### D. All the couplings are same order

Finally, we consider the case where all couplings are of the same order. We choose the representative values of the couplings  $a = -b = |g_{tu}^L| = 0.239$ , and  $c = d = 0.148$ . Again this value for  $g_{tu}^L$  satisfies the  $|\Delta_d|$  constraint but not the phase  $\phi_d^\Delta$  constraints from  $B_d$  mixing (see Fig. 2). In Fig. 6, we show the  $M_{t\bar{t}}$  distribution for the  $t\bar{t}$  observables  $A_{FB}^{t\bar{t}}$ , and  $\sigma_{t\bar{t}}$ . We note that  $A_{FB}^{t\bar{t}}$  can be explained within one  $\sigma$  error of its measurement for  $M_{t\bar{t}} > 450$  GeV. The distribution  $d\sigma_{t\bar{t}}/dM_{t\bar{t}}$  is also consistent with the measurements. Similar results are obtained with  $a = b = |g_{tu}^R| = 0.245$ , and  $c = d = 0.148$  as shown in Fig. 7. The conclusion is that the inclusion of the tensor couplings does not have a significant effect on the top  $A_{FB}$  and can only slightly lower the values of the couplings  $a$  and  $b$  relative to their values in the pure case, with no tensor couplings, discussed earlier. The presence of the tensor couplings may have an important impact on the polarization measurement in  $t\bar{t}$  production [75].



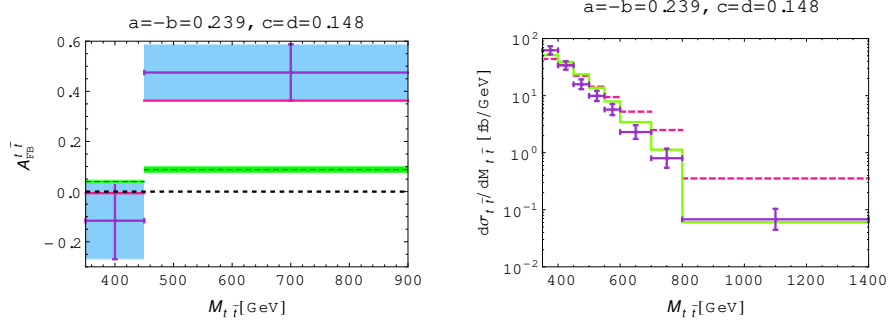


FIG. 6:  $M_{t\bar{t}}$  distributions of  $A_{FB}^{t\bar{t}}$  and  $d\sigma_{t\bar{t}}/dM_{t\bar{t}}$  [in fb/GeV]. Pink lines: the SM with  $Z'$  exchange prediction for ( $a = -b = 0.239$ ,  $c = d = 0.148$ ). The same conventions as in Fig. 4 used for other lines.

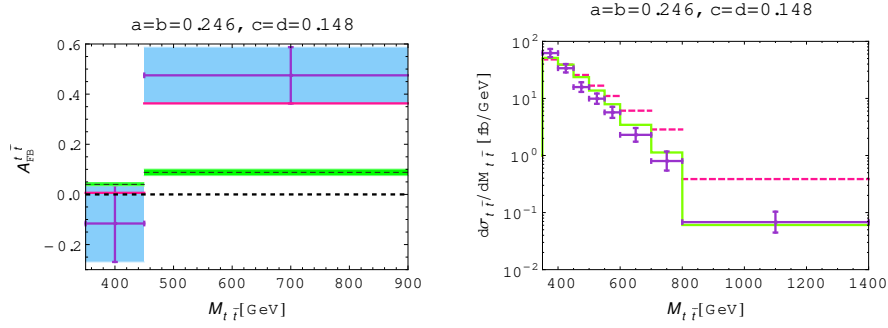


FIG. 7:  $M_{t\bar{t}}$  distributions of  $A_{FB}^{t\bar{t}}$  and  $d\sigma_{t\bar{t}}/dM_{t\bar{t}}$  [in fb/GeV]. Pink lines: the SM with  $Z'$  exchange prediction for ( $a = b = 0.245$ , and  $c = d = 0.148$ ). The same conventions as in Fig. 4 used for other lines.

### III. $t \rightarrow uZ'$ BRANCHING RATIO

In this section we consider the decay width for  $t \rightarrow uZ'$ . The decay width with the most general  $tuZ'$  coupling is given as,

$$\Gamma(t \rightarrow uZ') = \frac{1}{16\pi m_t} \left(1 - \frac{m_{Z'}^2}{m_t^2}\right) \left(\frac{m_t^2}{m_{Z'}^2} - 1\right) \left[ (m_t^2 + 2m_{Z'}^2)(a^2 + b^2) - 6m_{Z'}^2(ac - bd) + m_{Z'}^2 \left(\frac{m_{Z'}^2}{m_t^2} + 2\right)(c^2 + d^2) \right]. \quad (21)$$

Branching ratio is defined as

$$BR_{tuZ'} = \frac{\Gamma[t \rightarrow uZ']}{\Gamma[m_t]}. \quad (22)$$

For the top width we use  $\Gamma(m_t) \approx \Gamma(t \rightarrow bW)$  which is given by,

$$\Gamma(t \rightarrow bW) = \frac{G_F}{8\pi\sqrt{2}} |V_{tb}|^2 m_t^3 \left(1 - \frac{m_W^2}{m_t^2}\right) \left(1 + \frac{m_W^2}{m_t^2} - 2\frac{m_W^4}{m_t^4}\right). \quad (23)$$

In Fig. 8 we show the variation of  $t \rightarrow uZ'$  branching ratio with  $M_{Z'}$  for different couplings. For couplings  $a = \pm b = 0.257$ , and  $c = d = 0$  (red dashed line), we get  $BR_{tuZ'} \sim 6\%$  at  $m_t = 172.5$  GeV, for  $a = -b = 0.239$ ,  $c = -d = 0.148$  (blue dashed line),  $BR_{tuZ'}$  is 6.9%, and for  $a = b = 0.246$ ,  $c = d = 0.148$  (pink dashed line),  $BR_{tuZ'}$  is 7.2%. These branching ratios may be observable at the LHC [58].

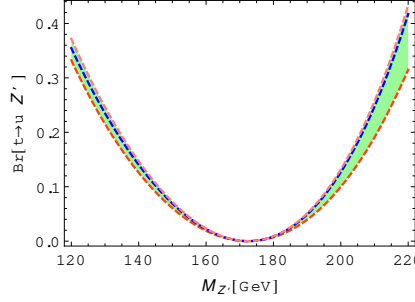


FIG. 8:  $BR_{Z'}$  vs  $M_{Z'}$ . Red dashed line is for  $a = \pm b = 0.257$ , and  $c = d = 0$ . Blue dashed line is for  $a = -b = 0.239$ ,  $c = -d = 0.148$ . Pink dashed line is for  $a = b = 0.246$ ,  $c = d = 0.148$ .

#### IV. CONCLUSION

A large forward-backward asymmetry in  $t\bar{t}$  production, about a  $3.4\sigma$  away from the SM prediction, has been reported by the CDF collaboration. A  $Z'$  with flavor-changing  $tuZ'$  coupling can explain this anomaly. In this work we considered  $B_{d,s}$  constraints on the  $tq'Z'$  couplings ( $q' = u, t$ ). These constraints resulted from the bounds on the effective  $b(s, d)Z'$  vertices generated from vertex corrections involving the  $tuZ'$  couplings. We found that the right-handed couplings were generally not tightly constrained but the left-handed couplings were tightly bound from the  $B_{d,s}$  mixing data. We then considered the most general  $tuZ'$  coupling including tensor terms and found that the tensor terms did not affect the top  $A_{FB}$  in a significant manner. Finally we computed the branching ratio for the  $t \rightarrow uZ'$  transition and found it to be in the percentage range.

**Acknowledgments:** This work was financially supported by the US-Egypt Joint Board on Scientific and Technological Co-operation award (Project ID: 1855) administered by the US Department of Agriculture.

#### Appendix A: Functions in scattering amplitudes

For the scattering amplitudes calculation in  $t\bar{t}$  center-of-mass frame, we choose the relevant coordinates of particle momenta as

$$\begin{aligned} p_{q,\bar{q}} &= \frac{\hat{s}}{2}(1, 0, 0, \pm 1), \\ p_{t,\bar{t}} &= \frac{\hat{s}}{2}(1, \pm\beta_t \sin\theta, 0, \pm\beta_t \cos\theta). \end{aligned} \quad (A1)$$

With this choice and assume all the couplings in Eq. (4) to be real, we obtain the functions  $f_i$  in the scattering amplitude in Eq. (18) as

$$\begin{aligned} f_1 &= \frac{\hat{s}}{2} \left[ 8 \left( 2a^2 + 2b^2 + ac - c^2 + 3bd + d^2 \right) \frac{m_t^2}{\hat{s}} + 2 \left( 2a^2(1 + c_\theta)^2 + 2b^2(1 + c_\theta)^2 \right. \right. \\ &\quad \left. \left. + bd(-7 + 4c_\theta + 6c_\theta^2 - 3\beta_t^2) - (c^2 - d^2)(-1 + 3c_\theta^2 - 2\beta_t^2) + ac(-1 + \beta_t^2) \right) \right. \\ &\quad \left. - \left( (-1 + c_\theta)(c^2 - d^2)(-1 + 2c_\theta + c_\theta^2 - 2\beta_t^2)\hat{s}^2 \right) \frac{\hat{s}}{m_t^2} \right], \\ f_2 &= - \left( \frac{m_t^2}{\hat{t}} \right) \hat{s}(a^2 + b^2) \left[ (-1 + c_\theta)^2 + \frac{4m_t^2}{\hat{s}} \right]. \end{aligned} \quad (A2)$$

$$\begin{aligned}
f_3 = & \frac{1}{16} \hat{s}^2 \left[ 32(a^4 + b^4) \left( 3 + 2c_\theta + c_\theta^2 + 2\beta_t^2 \right) + \frac{1}{m_t^4} (c^4 + d^4) \left( 32(9 - 2c_\theta + c_\theta^2) m_t^4 \right. \right. \\
& + 32(-5 + 3c_\theta + c_\theta^2 + c_\theta^3) m_t^2 \hat{s} + \hat{s}^2 (5 - 2c_\theta^2 + \beta_t^2 - c_\theta(3 + \beta_t^2))^2 \Big) + 128a^3 c \left( -2c_\theta + c_\theta^2 + \beta_t^2 \right) \\
& - \frac{1}{m_t^4} 2c^2 d^2 \left( -32(-5 + 3c_\theta + c_\theta^2 + c_\theta^3) m_t^2 \hat{s} + 32m_t^4 (-11 + 6c_\theta + c_\theta^2 - 4\beta_t^2) \right. \\
& - \hat{s}^2 (5 - 2c_\theta^2 + \beta_t^2 - c_\theta(3 + \beta_t^2))^2 \Big) + \frac{16}{m_t^2} ac \left( 8b^2 m_t^2 (-2 + 2c_\theta + 3c_\theta^2 - 3\beta_t^2) \right. \\
& + c^2 (-1 + c_\theta) (8(-3 + c_\theta) m_t^2 + \hat{s} (5 + 2c_\theta^2 - 3\beta_t^2 - c_\theta(3 + \beta_t^2))) - d^2 (8m_t^2 (-5 + 8c_\theta + c_\theta^2 - 4\beta_t^2) \\
& - (-1 + c_\theta) \hat{s} (5 + 2c_\theta^2 - 3\beta_t^2 - c_\theta(3 + \beta_t^2))) \Big) + \frac{16}{m_t^2} b^2 \left( c^2 (2m_t^2 (-11 - 2c_\theta + 5c_\theta^2 - 8\beta_t^2) \right. \\
& - (-1 + c_\theta) \hat{s} (5 + 3\beta_t^2 + c_\theta(7 + \beta_t^2))) - d^2 (4m_t^2 (7 - 2c_\theta + 2c_\theta^2 + \beta_t^2) \\
& + (-1 + c_\theta) \hat{s} (5 + 3\beta_t^2 + c_\theta(7 + \beta_t^2))) \Big) + \frac{16}{m_t^2} a^2 \left( 4b^2 m_t^2 (1 + 6c_\theta + 3c_\theta^2 - 2\beta_t^2) \right. \\
& - d^2 (2m_t^2 (3 + 18c_\theta + 3c_\theta^2 - 8\beta_t^2) + (-1 + c_\theta) \hat{s} (5 + 3\beta_t^2 + c_\theta(7 + \beta_t^2))) \\
& \left. \left. + c^2 (5\hat{s} + 4m_t^2 \beta_t^2 + 3\hat{s}\beta_t^2 - 2c_\theta(24m_t^2 + \hat{s}(-1 + \beta_t^2)) + c_\theta^2(12m_t^2 - \hat{s}(7 + \beta_t^2))) \right) \right], \\
f_4 = & -\frac{1}{2} \left( \frac{m_t^2}{\hat{t}} \right) \hat{s} \left[ 32(a^4 + b^4 + 2a^3 c + 2ab^2 c + a^2(2b^2 + c^2) - b^2 d^2) m_t^2 + 8(-3 + 2c_\theta + c_\theta^2) \right. \\
& \left. (a^3 c + ab^2 c + a^2 c^2 - b^2 d^2) \hat{s} + \frac{1}{m_t^2} (-1 + c_\theta)^2 (a^2 c^2 - b^2 d^2) \hat{s}^2 (5 + 2c_\theta + \beta_t^2) \right], \\
f_5 = & \left( \frac{m_t^2}{\hat{t}} \right)^2 \hat{s}^2 (a^2 + b^2)^2 (-1 + c_\theta)^2.
\end{aligned} \tag{A3}$$

- 
- [1] T. Aaltonen *et al.* [CDF Collaboration], arXiv:1101.0034 [hep-ex].
- [2] J. H. Kuhn and G. Rodrigo, *Phys.Rev.Lett.* **81** (1998) 49–52, [hep-ph/9802268].
- [3] J. H. Kuhn and G. Rodrigo, *Phys.Rev.* **D59** (1999) 054017, [hep-ph/9807420].
- [4] M. Bowen, S. Ellis, and D. Rainwater, *Phys.Rev.* **D73** (2006) 014008, [hep-ph/0509267].
- [5] L. G. Almeida, G. F. Sterman, and W. Vogelsang, *Phys.Rev.* **D78** (2008) 014008, [arXiv:0805.1885 [hep-ph]].
- [6] D0 Collaboration, V. Abazov *et. al.*, *Phys.Rev.Lett.* **100** (2008) 142002, [arXiv:0712.0851 [hep-ex]].
- [7] T. Aaltonen *et al.* [CDF Collaboration], Conf. Note 9913 (2009);
- [8] U. Langenfeld, S. Moch, and P. Uwer, *Phys. Rev. D.* **80**, 054009 (2009). [arXiv:0906.5273[hep-ph]].
- [9] M. Cacciari *et al.*, *JHEP* **09**, 127 (2008). [arXiv:0804.2800[hep-ph]].
- [10] N. Kidonakis and R. Vogt, *Phys. Rev. D.* **78**, 074005 (2008). [arXiv:0805.3844 [hep-ph]].
- [11] V. Ahrens, A. Ferroglia, M. Neubert, B. D. Pecjak and L. Li, *JHEP* **09**, 097 (2010). [arXiv:1003.5827[hep-ph]].
- [12] L. Sehgal and M. Wanninger, *Phys.Lett.* **B200** (1988) 211.
- [13] J. Bagger, C. Schmidt, and S. King, *Phys.Rev.* **D37** (1988) 1188.
- [14] P. Ferrario and G. Rodrigo, *Phys.Rev.* **D80** (2009) 051701, [arXiv:0906.5541[hep-ph]].
- [15] P. H. Frampton, J. Shu, and K. Wang, *Phys. Lett.* **B683** (2010) 294–297, [arXiv:0911.2955 [hep-ph]].
- [16] D. W. Jung, P. Ko, J. S. Lee and S. H. Nam, *Phys. Lett.* **B691** (2010) 238–242, [arXiv:0912.1105 [hep-ph]].
- [17] R. Chivukula, E. H. Simmons, and C.-P. Yuan, *Phys.Rev.* **D82** (2010) 094009, [arXiv:1007.0260 [hep-ph]].
- [18] A. Djouadi, G. Moreau, F. Richard, and R. K. Singh, *Phys.Rev.* **D82** (2010) 071702, [arXiv:0906.0604 [hep-ph]].
- [19] M. Bauer, F. Goertz, U. Haisch, T. Pfoh, and S. Westhoff, *JHEP* **1011** (2010) 039, [arXiv:1008.0742 [hep-ph]].
- [20] E. Alvarez, L. Da Rold, and A. Szyrkman, arXiv:1011.6557 [hep-ph].
- [21] C.-H. Chen, G. Cvetič, and C. Kim, *Phys.Lett.* **B694** (2011) 393–397, [arXiv:1009.4165 [hep-ph]].
- [22] C. Delaunay, O. Gedalia, S. J. Lee, G. Perez, E. Ponton, arXiv:1101.2902 [hep-ph].

- [23] Y. Bai, J. L. Hewett, J. Kaplan, T. G. Rizzo, *JHEP* **1103** (2011) 003, [arXiv:1101.5203 [hep-ph]].
- [24] A. R. Zerwekh, arXiv:1103.0956 [hep-ph].
- [25] E. R. Barreto, Y. A. Coutinho, J. S. Borges, arXiv:1103.1266 [hep-ph].
- [26] A. Djouadi, G. Moreau, F. Richard, arXiv:1105.3158 [hep-ph].
- [27] R. Barcelo, A. Carmona, M. Masip, J. Santiago, arXiv:1105.3333 [hep-ph].
- [28] S. Westhoff, arXiv:1105.4624 [hep-ph].
- [29] U. Haisch, S. Westhoff, arXiv:1106.0529 [hep-ph].
- [30] E. Gabrielli, M. Raidal, arXiv:1106.4553 [hep-ph].
- [31] S. Jung, H. Murayama, A. Pierce, and J. D. Wells, *Phys. Rev.* **D81** (2010) 015004, [arXiv:0907.4112 [hep-ph]].
- [32] K. Cheung, W.-Y. Keung, and T.-C. Yuan, *Phys. Lett.* **B682** (2009) 287–290, [arXiv:0908.2589 [hep-ph]].
- [33] J. Shu, T. M. P. Tait, and K. Wang, *Phys. Rev.* **D81** (2010) 034012, [arXiv:0911.3237 [hep-ph]].
- [34] I. Dorsner, S. Fajfer, J. F. Kamenik, and N. Kosnik, *Phys. Rev.* **D81** (2010) 055009, [arXiv:0912.0972 [hep-ph]].
- [35] A. Arhrib, R. Benbrik, and C.-H. Chen, *Phys. Rev.* **D82** (2010) 034034, [arXiv:0911.4875 [hep-ph]].
- [36] V. Barger, W.-Y. Keung, and C.-T. Yu, *Phys. Rev.* **D81** (2010) 113009, [arXiv:1002.1048 [hep-ph]].
- [37] S. K. Gupta, G. Valencia, *Phys. Rev.* **D82**, 035017 (2010). [arXiv:1005.4578 [hep-ph]].
- [38] B. Xiao, Y.-k. Wang, and S.-h. Zhu, *Phys. Rev.* **D82** (2010) 034026, [arXiv:1006.2510 [hep-ph]].
- [39] S. K. Gupta, arXiv:1011.4960 [hep-ph].
- [40] K. Cheung and T.-C. Yuan, arXiv:1101.1445 [hep-ph].
- [41] J. Cao, L. Wang, L. Wu, J. M. Yang, [arXiv:1101.4456 [hep-ph]].
- [42] E. L. Berger, Q. -H. Cao, C. -R. Chen, C. S. Li, H. Zhang, arXiv:1101.5625 [hep-ph].
- [43] V. Barger, W. -Y. Keung, C. -T. Yu, arXiv:1102.0279 [hep-ph].
- [44] B. Grinstein, A. L. Kagan, M. Trott, J. Zupan, arXiv:1102.3374 [hep-ph].
- [45] K. M. Patel, P. Sharma, arXiv:1102.4736 [hep-ph].
- [46] S. Jung, A. Pierce, J. D. Wells, arXiv:1103.4835 [hep-ph].
- [47] M. R. Buckley, D. Hooper, J. Kopp, E. Neil, arXiv:1103.6035 [hep-ph].
- [48] J. Shu, K. Wang, G. Zhu, arXiv:1104.0083 [hep-ph].
- [49] A. Rajaraman, Z. Surujon, T. M. P. Tait, arXiv:1104.0947 [hep-ph].
- [50] J. A. Aguilar-Saavedra, M. Perez-Victoria, arXiv:1104.1385 [hep-ph].
- [51] C. Degrande, J. M. Gerard, C. Grojean, F. Maltoni, G. Servant, arXiv:1104.1798 [hep-ph].
- [52] X. P. Wang, Y. K. Wang, B. Xiao, J. Xu, S. h. Zhu, arXiv:1104.1917 [hep-ph].
- [53] A. E. Nelson, T. Okui, T. S. Roy, arXiv:1104.2030 [hep-ph].
- [54] S. Jung, A. Pierce, J. D. Wells, arXiv:1104.3139 [hep-ph].
- [55] D. W. Jung, P. Ko, J. S. Lee, arXiv:1104.4443 [hep-ph].
- [56] K. S. Babu, M. Frank, S. K. Rai, arXiv:1104.4782 [hep-ph].
- [57] J. A. Aguilar-Saavedra, M. Perez-Victoria, arXiv:1105.4606 [hep-ph].
- [58] M. I. Gresham, I. W. Kim and K. M. Zurek, arXiv:1103.3501 [hep-ph].
- [59] S. L. Glashow and S. Weinberg, *Phys. Rev. D* **15**, 1958 (1977); E. A. Paschos, *Phys. Rev. D* **15**, 1966 (1977).
- [60] See for e.g. S. Baek, A. Datta, P. Hamel, O. F. Hernandez and D. London, *Phys. Rev. D* **72**, 094008 (2005) [arXiv:hep-ph/0508149]. S. Baek, P. Hamel, D. London, A. Datta and D. A. Suprun, *Phys. Rev. D* **71**, 057502 (2005) [arXiv:hep-ph/0412086]; A. Datta, *Phys. Rev. D* **66**, 071702 (2002) [arXiv:hep-ph/0208016]; A. Datta, X. G. He and S. Pakvasa, *Phys. Lett. B* **419**, 369 (1998) [arXiv:hep-ph/9707259].
- [61] T. Han, R. D. Peccei and X. Zhang, *Nucl. Phys. B* **454**, 527 (1995), [arXiv:hep-ph/9506461]; T. Han, K. Whisnant, B. L. Young and X. Zhang, *Phys. Rev. D* **55**, 7241 (1997), [arXiv:hep-ph/9603247]. T. Han, K. Whisnant, B. L. Young and X. Zhang, *Phys. Lett. B* **385**, 311 (1996), [arXiv:hep-ph/9606231];
- [62] P. J. Fox, J. Liu, D. Tucker-Smith and N. Weiner, arXiv:1104.4127 [hep-ph].
- [63] A. Datta and D. London, *Int. J. Mod. Phys. A* **19**, 2505 (2004), [arXiv:hep-ph/0303159]. A. Datta, M. Duraissamy and D. London, arXiv:1103.2442 [hep-ph].
- [64] A. Datta and X. Zhang, *Phys. Rev. D* **55**, 2530 (1997), [arXiv:hep-ph/9611247].
- [65] A. Lenz *et al.*, *Phys. Rev. D* **83**, 036004 (2011), [arXiv:1008.1593 [hep-ph]].
- [66] A. Abulencia *et al.* [CDF Collaboration], *Phys. Rev. Lett.* **97**, 242003 (2006), [arXiv:hep-ex/0609040].
- [67] V. M. Abazov *et al.* [D0 Collaboration], *Phys. Rev. Lett.* **101**, 241801 (2008), [arXiv:0802.2255 [hep-ex]].

- [68] D. Asner *et al.* [The Heavy Flavor Averaging Group] , arXiv:1010.1589 [hep-ex].
- [69] A. Datta and M. Duraissamy, Phys. Rev. D **81**, 074008 (2010), [arXiv:0912.4785 [hep-ph]].
- [70] C. H. Chen, Sandy S. C. Law and Run-Hui Li, arXiv:1104.1497 [hep-ph].
- [71] H. L. Lai *et al.* [ CTEQ Collaboration ], Eur. Phys. J. **C12**,375-392 (2000), [hep-ph/9903282].
- [72] A. D. Martin, W. J. Stirling, R. S. Thorne, G. Watt, Eur. Phys. J. **C63**,189-285 (2009), [arXiv:0901.0002 [hep-ph]].
- [73] Q. H. Cao, D. McKeen, J. L. Rosner, G. Shaughnessy and C. E. M. Wagne, Phys. Rev. D. **81**,114004 (2010), [arXiv:1003.3461 [hep-ph]].
- [74] T. Aaltonen *et al.* [CDF Collaboration], Phys. Rev. Lett. **102**, 222003 (2009). [arXiv: 0903.2850[hep-ex]].
- [75] D. -W. Jung, P. Ko, J. S. Lee, arXiv:1011.5976 [hep-ph]; D. Choudhury, R. M. Godbole, S. D. Rindani, and P. Saha, arXiv:1012.4750.